Chimera states in time-varying complex networks

Arturo Buscarino,[1] Mattia Frasca,[1,*] Lucia Valentina Gambuzza,[1] and Philipp Hövel[2,3]
[1]*DIEEI, Università degli Studi di Catania, Catania, Italy*
[2]*Institut für Theoretische Physik, Technische Universität Berlin, Hardenbergstraße 36, 10623 Berlin, Germany*
[3]*Bernstein Center for Computational Neuroscience Berlin, Humboldt-Universität zu Berlin, Philippstraße 13, 10115 Berlin, Germany*
(Received 19 December 2014; published 26 February 2015)

Chimera states have been recently found in a variety of different coupling schemes and geometries. In most cases, the underlying coupling structure is considered to be static, while many realistic systems display significant temporal changes in the pattern of connectivity. In this work we investigate a time-varying network made of two coupled populations of Kuramoto oscillators, where the links between the two groups are considered to vary over time. As a main result we find that the network may support stable, breathing, and alternating chimera states. We also find that, when the rate of connectivity changes is fast, compared to the oscillator dynamics, the network may be described by a low-dimensional system of equations. Unlike in the static heterogeneous case, the onset of alternating chimera states is due to the presence of fluctuations, which may be induced either by the finite size of the network or by large switching times.

DOI: 10.1103/PhysRevE.91.022817 PACS number(s): 89.75.−k, 05.45.Xt

I. INTRODUCTION

The first evidence of chimera states dates back to 2002 [1], when Kuramoto and Battogtokh, studying a system of identical phase oscillators coupled in a nonlocal way, discovered the onset of a counterintuitive behavior: the oscillators split into two coexisting subpopulations, one coherent and one incoherent. Since that first report, the phenomenon attracted a lot of interest leading to the discovery of chimera states in a variety of systems (phase oscillators [1–6], neurons [7,8], chemical units [9], and chaotic units [10,11]). While chimera states were initially observed only in systems with nonlocal coupling (one-dimensional rings [1,2] and two-dimensional systems [3,5,6]) and for pure phase dynamics, the results of recent works pointed out the appearance of chimera states also in systems with global coupling or with no negligible amplitude dynamics [7,12–16].

A structure particularly relevant for our study is the one formed by two coupled populations where each oscillator is equally coupled to all the others in its group, and less strongly to those in the other group [4]. Despite the symmetry of the coupling structure, an asymmetric behavior—with one population displaying synchronized oscillations and the other exhibiting incoherence—emerges in this network. The incoherent population may either show a constant level of desynchronization (*stable chimera*) or an oscillating one (*breathing chimera*). Notably, when the intrinsic frequencies of oscillators are not homogeneous, an *alternating chimera*, where the two populations alternate in the level of synchrony, is observed [17]. This behavior mirrors unihemispheric sleep, where sleep alternates between the two hemispheres with one half of the brain awake with desynchronized neuronal activity and the other sleeping and synchronized [18–20]. Alternating chimera states have been also found in coupled populations of forced oscillators [21], in time-delayed systems [22], and in isotropic oscillatory media with nonlinear uniform global coupling [23]. The onset of stable and breathing chimera states is not limited to two populations, but is found also in systems formed by more than two coupled populations [24,25].

In recent works, the concept of chimera states has been generalized to include other types of symmetry breaking solutions and new terms have been coined: *amplitude-mediated chimera* displaying temporal variations of the amplitude in the incoherent population [12]; *amplitude chimera*, that is, a chimera behavior in the oscillators amplitudes rather than their phases [10,11]; *chimera death* [14], characterized by coexistence of spatially coherent and incoherent oscillation death; and *chimera states with quiescent and synchronous domains* (QSCS), where synchronization coexists with spatially patterned oscillation death [7,8]. In parallel to theoretical investigations, experimental studies have demonstrated the existence of chimera states in real systems. In [26] chimera states have been revealed in a coupled map lattice made of a liquid-crystal spatial light modulator; in [9] a system of coupled Belousov-Zhabotinsky oscillators has shown chimera behaviors such as phase-cluster states; and in [27] chimera states have been observed in a set of metronomes placed on two weakly coupled swings. An experimental evidence of QSCS is reported in [8] for a system of electronic circuits with neuronlike spiking dynamics.

Most of the works on chimera states assume that the connection structure is static. However, in many systems (for example, communication, ecological, social, and contact networks) links are not always active and the connectivity between units changes during time with a rate ranging from slow to fast [28]. The dynamics of the systems interacting through a network can be significantly affected by the link activity. For this reason, the pattern of link activation is explicitly taken into account as an element of the system in the study of time-varying or temporal networks [28]. The dynamics of time-varying networks are characterized by the presence of two time scales (those of the dynamical process and that of the link activation) and by the rule (which can be either deterministic or stochastic) defining the connectivity changes in time. In several works [29–31], to account for sporadic intermittent interactions, time-dependent connections are introduced by switching on or off, at a fixed frequency, a

*Corresponding author: mfrasca@diees.unict.it

subset or the whole set of the edges of a network. For this setting, an analytical approach for global synchronization is derived in the limit of fast switching. In this paper we use this framework to study the onset of chimera states in a time-varying network. In particular, we consider a system made of two coupled populations with strong, time-independent links within each group and less strong interconnections between them modeled by time-dependent edges. We found that the system may exhibit stable, breathing, and alternating chimera states. Alternating chimera states are found when the fluctuations due to the stochastic switching of the connections are not negligible.

The rest of this paper is organized as follows: Section II introduces the model equations and network structure and presents a bifurcation diagram. Section III discusses a low-dimensional set of reduced equations to illustrate the mechanism of switching. Section IV addresses questions related to the size of the populations. Finally, we summarize the results in Sec. V.

II. A SYSTEM OF TWO COUPLED POPULATIONS WITH TIME-VARYING INTERACTIONS

We study a pair of oscillator populations [32,33], and consider the coupling between groups changing as a function of time. Each population σ (with $\sigma = 1,2$) consists of N_σ identical phase oscillators. Within each population the oscillators are globally coupled with links fixed in time and of weight μ, while the coupling between the two populations is time varying. The inter-population links are randomly switched on or off at fixed equally spaced time intervals of length τ. During each time interval, every possible connection between two nodes in different groups is turned on, with probability p_{switch} and weight equal to one, independently of the other links, and independently of whether or not it has been turned on during the previous time interval. This leads to an interpopulation connectivity which is a time-varying matrix given by a random sequence of Erdős-Rényi graphs with average in-degree $p_{\text{switch}} N_\sigma$. The system of two interacting populations is described by

$$\frac{d}{dt}\theta_i^\sigma = \omega + \sum_{\sigma'=1}^{2} \frac{1}{N_{\sigma'}} \sum_{j=1}^{N_{\sigma'}} K_{ij}^{\sigma\sigma'}(t) \sin\left(\theta_j^{\sigma'} - \theta_i^\sigma - \alpha\right), \quad (1)$$

where θ_i^σ is the phase of oscillator i in population σ, ω is the intrinsic frequency (equal for all the oscillators, fixed without loss of generality at $\omega = 1$), α is the phase lag, and $K_{ij}^{11}(t) = K_{ij}^{22}(t) = \mu > 0\,\forall t$. $\mathbf{K}^{12}(t) = [\mathbf{K}^{21}(t)]^T$ are stochastic matrices whose elements are defined as $K_{ij}^{12}(t) = K_{ji}^{21}(t) = s_{ij}(q)$ for $(q-1)\tau < t < q\tau$ with

$$s_{ij}(q) = \begin{cases} 1, & \text{with probability } p_{\text{switch}}, \\ 0, & \text{with probability } 1 - p_{\text{switch}}, \end{cases} \quad (2)$$

where $q \in \mathcal{N}^+$ defines the number of switching intervals, each of length τ.

To monitor coherence in each population, two separate Kuramoto order parameters are considered:

$$r_\sigma(t) = |\langle e^{\iota\theta_i(t)}\rangle_\sigma|, \quad (3)$$

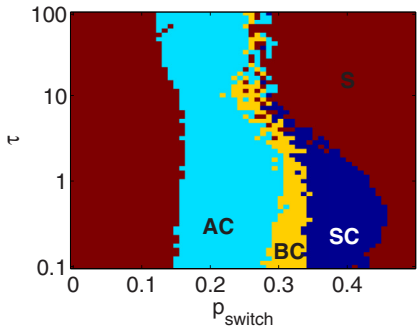

FIG. 1. (Color online) Bifurcation map with respect to the switching probability p_{switch} and to the length of the switching interval τ. The population size is $N = 100$, the coupling strength within each group is fixed to $\mu = 0.6$, the oscillators frequency $\omega = 1$, and the phase lag $\alpha = 1.5$. The regions are labeled according to the behavior observed: S synchronization; SC stable chimera; BC breathing chimera; and AC alternating chimera.

with $\sigma = 1,2$ and $\iota = \sqrt{-1}$. $\langle\cdot\rangle_\sigma$ denotes the average over all elements in population σ.

To illustrate the effect of the switching of the interpopulation links, we discuss the behavior of a network with $N_1 = N_2 = N = 100$ oscillators by varying the values of the parameters ruling the switching, that is, the probability p_{switch} and the length τ of the time intervals. The bifurcation diagram, shown in Fig. 1, reveals the onset of different types of chimera states in a large region of the parameter space $(p_{\text{switch}}, \tau)$. The region labeled as S is characterized by synchronization of both populations, $r_1 = r_2 \simeq 1$. All the other regions indicate coexistence of synchronization with a chimera state. These are illustrated in Fig. 2, where the evolution of the two Kuramoto order parameters is reported for selected values of p_{switch} with τ fixed to $\tau = 0.1$. Stable chimeras are found in the region SC (cf. Fig. 1) and are characterized by one coherent population, showing synchronized oscillations and an order parameter close to one [population 2 in Fig. 2(a)] and one desynchronized (population 1). The phase coherence for the desynchronized population remains approximately constant. For breathing chimeras (region BC in Fig. 1), instead, the phase coherence of the desynchronized population is not constant, but pulsates [Fig. 2(b)]. Alternating chimera states appear in the region AC. These chimeras are characterized by alternating synchrony between the two populations [Fig. 2(c)]. While one population is nearly synchronized, the other displays a pulsating order parameter; the oscillators in the desynchronized population may then gain synchrony at the expense of the oscillators in the other population which lose synchrony. The behavior is found to alternate with either regular or irregular periods as a function of the value of p_{switch} and τ. To gain further insights about the alternating behavior of the Kuramoto order parameters, the average period of alternation $\langle T_p\rangle$ has been characterized. Figure 3 shows a typical scenario obtained for $p_{\text{switch}} = 0.2$, that is, a value for which any point $(p_{\text{switch}}, \tau)$ in Fig. 1 belongs to the AC region. The average period of alternation $\langle T_p\rangle$ exhibits a nonmonotonic behavior, with a first part where it slightly decreases as a function of τ. In this interval, the period of alternation is quite regular and distributed according to a Gaussian. Further increasing of τ

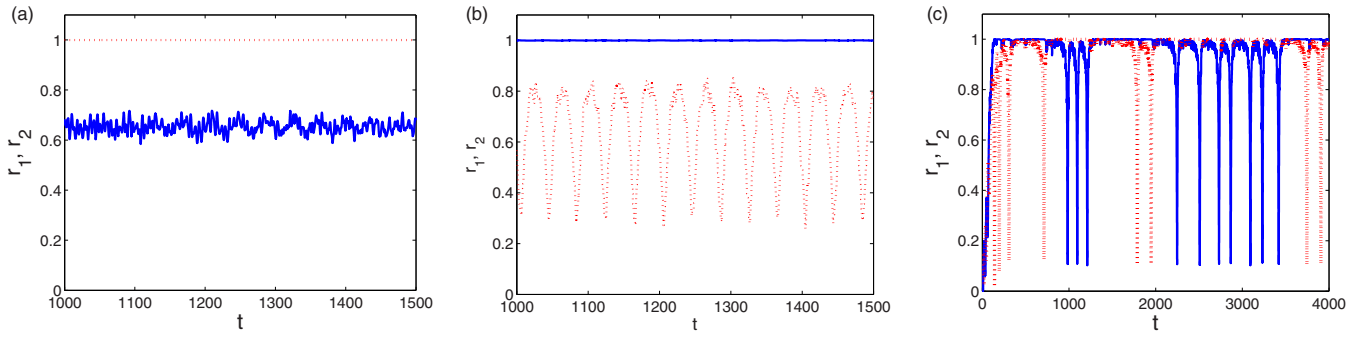

FIG. 2. (Color online) Time series of the two order parameters $r_1(t)$ (blue solid line) and $r_2(t)$ (red dotted line) for $\tau = 0.1$ and different values of the switching probability p_{switch}: (a) $p_{\text{switch}} = 0.38$; (b) $p_{\text{switch}} = 0.33$; and (c) $p_{\text{switch}} = 0.25$. Other parameters as in Fig. 1.

leads to an irregular behavior characterized by larger values of the average and a distribution of T_p which now spans several orders of magnitude (cf. inset for $\tau = 13.7$). After a peak around $\tau \approx 13$, the distribution remains long tailed but $\langle T_p \rangle$ becomes smaller. Very long periods of alternation are still probable in this region, but occur more rarely.

The presence of coexisting states makes the system behavior dependent on initial conditions. However, we have found that the appearance of chimera states in system (1) does not require particular initial conditions, whereas in other structures [1] the chimera states are observed starting from initial conditions close to the final state. Figure 1, for instance, has been obtained by assuming for each point of the diagram the same initial condition, generated by drawing values from a uniform random distribution in $[0, 2\pi]$.

Our findings reveal that, when the two populations are coupled with time-varying links, stable, breathing, and alternating chimeras are all observed for identical oscillators. Comparing this result with the analysis of patterns considering connectivity fixed in time, reported in [4] and [17], we note that, if the intrinsic frequencies are homogeneous, only stable and breathing chimeras appear [4], while the onset of alternating chimeras requires heterogeneity of the oscillators [17].

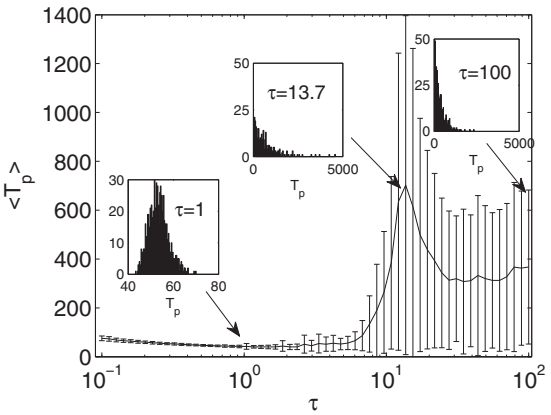

FIG. 3. Average period of alternation $\langle T_p \rangle$ as a function of the switching period τ for a population size of $N = 100$ and $p_{\text{switch}} = 0.2$. The other parameters are fixed as in Fig. 1. The insets show the distribution of the periods of alternation for selected values of τ. The error bars correspond to the standard deviation of T_p.

III. REDUCED EQUATIONS

In the thermodynamic limit of infinite system size, $N \to \infty$, many high-dimensional systems show low-dimensional dynamics. These systems may be reduced to a small set of ordinary differential equations for the study of the macroscopic evolution. This has been recently demonstrated for a system of globally coupled Kuramoto oscillators, which is reduced to a single first-order ordinary differential equation [34], and then generalized to assortative networks [35], time-varying topologies [36], and arbitrary number of communities [37,38]. In this section we write down a low-dimensional model for Eqs. (1) and show that this is able to explain the occurrence of stable and breathing chimeras in our system. The mechanism underlying the onset of alternating chimera states will be discussed in Sec. IV.

We first introduce a nonswitching system, obtained from Eq. (1) by considering a time-averaged connectivity:

$$\frac{d}{dt}\theta_i^\sigma = \omega + \sum_{\sigma'=1}^{2} \frac{\langle K_{ij}^{\sigma\sigma'} \rangle}{N_{\sigma'}} \sum_{j=1}^{N_{\sigma'}} \sin\left(\theta_j^{\sigma'} - \theta_i^\sigma - \alpha\right), \quad (4)$$

with

$$\langle K^{\sigma\sigma'} \rangle = \begin{cases} \mu, & \text{if} \quad \sigma = \sigma', \\ p_{\text{switch}}, & \text{if} \quad \sigma \neq \sigma'. \end{cases} \quad (5)$$

Under the assumption that the switching period is small, that is, the changes of the network topology operate on a time scale faster than the node dynamics, it is to be expected that the behavior of the switching system in Eq. (1) is close to that of the averaged system. This is also confirmed by several works investigating the effects of an increasing switching frequency in temporal networks [29–31,39].

By applying the Ott-Antonsen ansatz [34] to Eq. (4), the dynamics of the averaged system is then described in terms of the oscillator density distribution $f^\sigma(\theta)$. Omitting a detailed derivation, one obtains the following set of reduced equations:

$$\dot{\rho}_\sigma = \frac{1 - \rho_\sigma^2}{2} \sum_{\sigma'=1}^{2} \langle K^{\sigma\sigma'} \rangle \rho_{\sigma'} \sin(\phi_{\sigma'} - \phi_\sigma + \beta), \quad (6a)$$

$$\dot{\phi}_\sigma = \omega - \frac{1 + \rho_\sigma^2}{2\rho_\sigma} \sum_{\sigma'=1}^{2} \langle K^{\sigma\sigma'} \rangle \rho_{\sigma'} \cos(\phi_{\sigma'} - \phi_\sigma + \beta), \quad (6b)$$

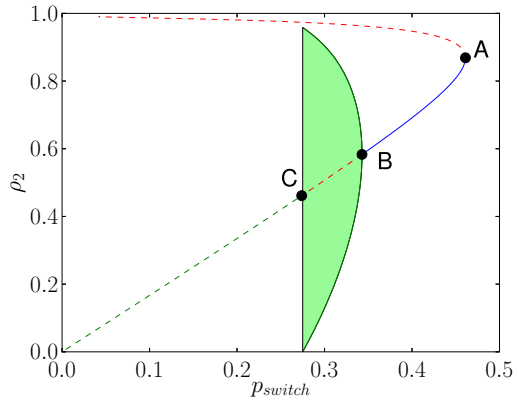

FIG. 4. (Color online) Bifurcation diagram of system (7) with respect to parameter p_{switch}. Solid (dashed line) curves indicate stable (unstable) fixed points. Green shading refers to a stable limit cycle. Points A, B, and C mark the saddle-node, Hopf, and homoclinic bifurcation, respectively. Parameters: $\mu = 0.6$ and $\alpha = 1.5$.

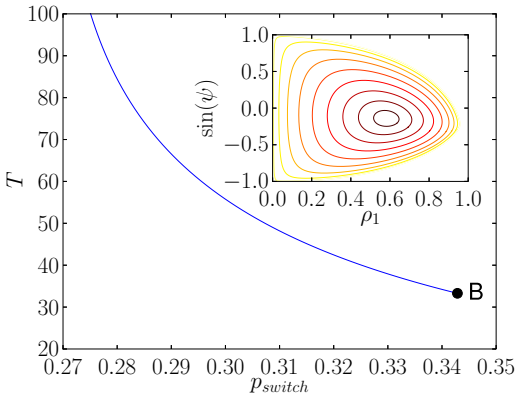

FIG. 5. (Color online) Period T of the limit cycle present in system (7) in dependence on p_{switch}. Point B marks the Hopf bifurcation. The inset shows the limit cycle in the $[\rho_1, \sin(\psi)]$ plane. The color gradient corresponds to the p_{switch} values (dark: larger, bright: smaller). Parameters: $\mu = 0.6$ and $\alpha = 1.5$.

where we used $\beta = \pi/2 - \alpha$. Defining the phase difference between the two populations $\psi = \phi_1 - \phi_2$ yields the following equations:

$$\dot{\rho}_1 = \frac{1-\rho_1^2}{2}[\mu\rho_1 \cos\alpha + p_{\text{switch}}\rho_2 \cos(-\psi - \alpha)], \tag{7a}$$

$$\dot{\rho}_2 = \frac{1-\rho_2^2}{2}[\mu\rho_2 \cos\alpha + p_{\text{switch}}\rho_1 \cos(\psi - \alpha)], \tag{7b}$$

$$\dot{\psi} = -\frac{1+\rho_1^2}{2}\left[\mu \sin\alpha + p_{\text{switch}}\frac{\rho_2}{\rho_1}\sin(\psi + \alpha)\right] + \frac{1+\rho_2^2}{2}\left[\mu \sin\alpha + p_{\text{switch}}\frac{\rho_1}{\rho_2}\sin(-\psi + \alpha)\right]. \tag{7c}$$

System (7) is studied with respect to the parameter $p_{\text{switch}} \in [0,0.5]$. Beyond the trivial equilibrium point (1,1,0), which represents global synchronization of the network, the system may have four further equilibria and two additional invariant limit cycles depending on p_{switch} as discussed below. Due to symmetry with respect to coordinates change $(\rho_1, \rho_2, \psi) \to (\rho_2, \rho_1, -\psi)$, it suffices to study only the equilibria on one of the planes $\rho_1 = 1$ or $\rho_2 = 1$.

Figure 4 depicts the bifurcation diagram of system (7) for $\rho_1 = 1$. Starting from $p_{\text{switch}} = 0.5$ and decreasing this parameter, we find a saddle-node bifurcation (point A in Fig. 4), a Hopf bifurcation (point B in Fig. 4), and a homoclinic bifurcation (point C in Fig. 4). The different regions in the bifurcation diagram correspond to the onset of different types of chimera states. For $p_{\text{switch}} \in [B, A]$ the system (7) has three stable equilibrium points, which correspond to global synchronization or stable chimeras in one of the two populations. For $p_{\text{switch}} \in [C, B]$ the system (7) has one stable equilibrium and—due to the symmetry mentioned above—two stable limit cycles, which give rise to a coexistence of global synchronization and breathing chimera states. The period of these limit cycles increases for decreasing p_{switch} (see Fig. 5) meaning that the period of the breathing chimera becomes longer as p_{switch} approaches the homoclinic bifurcation point. At the homoclinic bifurcation point C the limit cycles of system (7) collide and annihilate in a homoclinic bifurcation so that for $p_{\text{switch}} \in [0, C]$ only the trivial equilibrium (1,1,0) persists.

We find that the reduced equations (7) are effectively able to predict the behavior of the switching system for small τ and $p_{\text{switch}} \in [C, 0.5]$. Outside this region, alternating chimeras, not predicted by the reduced model, are found. As we will show in the next section, the discrepancy between the prediction and the behavior observed in Fig. 1 is not due to a failure of the reduced model, but reflects a difference between a finite and an infinite network.

System (7) has been numerically simulated for several values of p_{switch} and the results have been reported in Fig. 6, showing its phase portrait and the time evolution of ρ_1 and ρ_2. To better illustrate the coexistence of multiple attractors, three different initial conditions are considered in Figs. 6(a)–6(c). Figure 6(a), obtained for $p_{\text{switch}} = 0.38$, shows the coexistence of the equilibrium point (1,1,0) (synchronization of the two populations), and the two symmetrical equilibrium points in which either $\rho_1 = 1$ or $\rho_2 = 1$ (stable chimeras). Figure 6(b), obtained for $p_{\text{switch}} = 0.33$, shows an example of coexistence of the trivial equilibrium point (1,1,0), and stable limit cycles (breathing chimeras). Finally, Fig. 6(c) represents an example of the phase portrait obtained for a value of p_{switch} ($p_{\text{switch}} = 0.25$) smaller than the homoclinic bifurcation point C, where only the equilibrium (1,1,0) exists. The comparison between the behavior of the reduced model (7) and that of the switching system (1) shows that, for small τ and $p_{\text{switch}} \in [C, 0.5]$, the trajectory of the switching system is close to that of the averaged reduced model. For instance, for $p_{\text{switch}} = 0.38$ the phase portrait and the trajectories of the averaged reduced model, shown in Figs. 6(a) and 6(d), are in agreement with the stable chimera displayed by the switching system in Fig. 2(a). An agreement is also found in the case of breathing chimera states, observed in the reduced model for $p_{\text{switch}} \in [C, B]$. For example, for $p_{\text{switch}} = 0.33$ the state of the switching system [Fig. 2(b)] is a breathing chimera which is reproduced by the averaged reduced model [Figs. 6(b) and 6(e)].

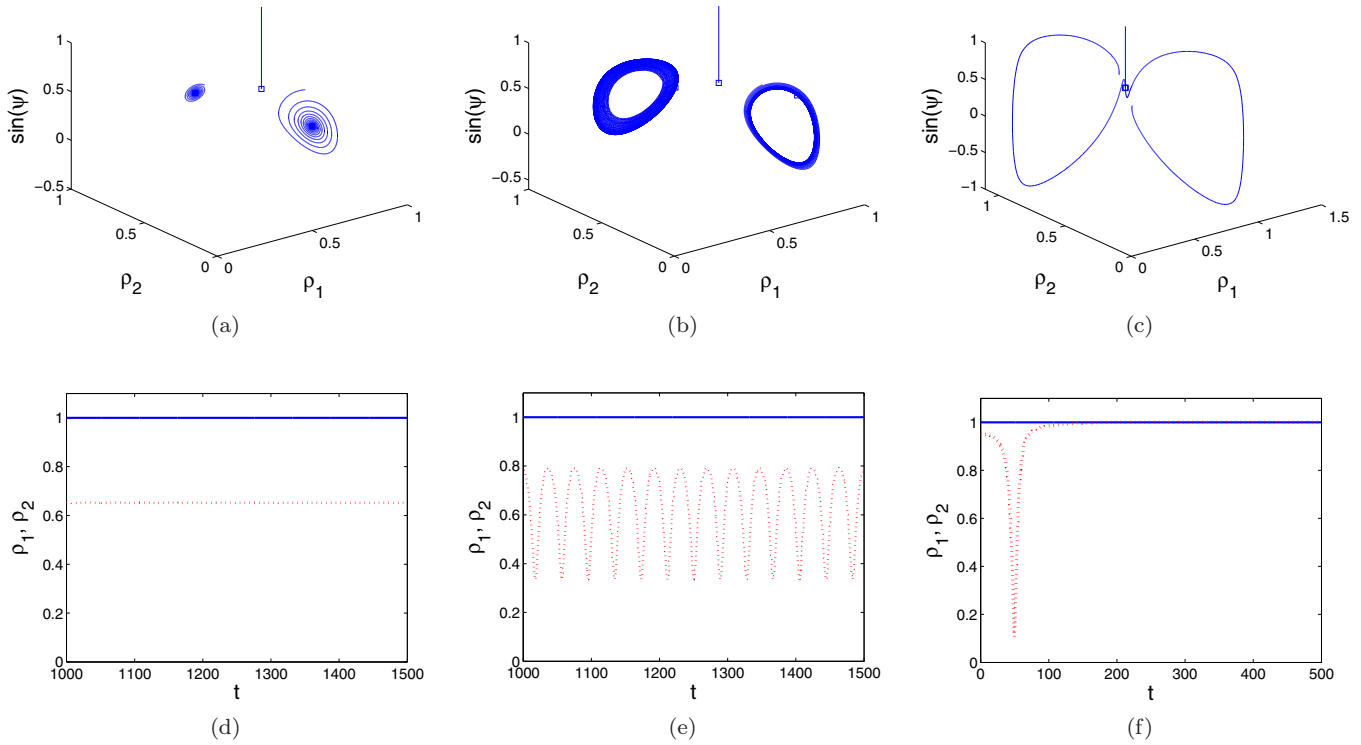

FIG. 6. (Color online) (a)–(c) Phase portrait of Eqs. (7) and (d)–(f) time evolution of ρ_1 (blue solid line) and ρ_2 (red dotted line) with parameters: (a) and (d) $p_{\text{switch}} = 0.38$; (b) and (e) $p_{\text{switch}} = 0.33$; and (c) and (f) $p_{\text{switch}} = 0.25$. Other parameters as in Fig. 4.

IV. ONSET OF ALTERNATING CHIMERAS

In this section we discuss the behavior in the region of parameter $p_{\text{switch}} \in [0, C]$. In this region the reduced model predicts that only global synchronization is possible. However, alternating chimera states are observed even for small switching intervals as shown in Fig. 1. The discrepancy is due to the finite size of the network under consideration, which counts $N = 100$ oscillators in each population.

To show that the model accurately predicts the absence of chimera states in this region in the thermodynamic limit, we have carried out simulations at increasing values of the network size and identified the region where alternating chimera states appear. We notice that this region depends on τ, but as predicted by the reduced model the one corresponding to small τ tends to shrink when the network size increases (Fig. 7). For large N alternating chimera states are still found for larger values of τ (cf. the inset of Fig. 7). We thus conjecture that the onset of chimera states is due to fluctuations and that the causes of these fluctuations are the finite size of the network and the large switching periods. In line with this, we have seen that: (i) when noise is added to the reduced model, an alternating behavior may be observed; and (ii) fluctuations increase when τ is increased or N decreased.

In the region $p_{\text{switch}} \in [0, C]$, due to the homoclinic bifurcation, the structure of the phase portrait of the reduced model is such that the trajectory, starting in a neighborhood of the only stable equilibrium point $(1, 1, 0)$, experiences a large excursion before returning to the equilibrium [Figs. 6(c) and 6(f)]. In the presence of fluctuations this may lead to a series of pulses in the evolution of the variables ρ_1 and ρ_2. To confirm this, simulations of the model (7) subject to an additive noise term are carried out. In particular, we have considered a stochastic term added to the averaged reduced system as follows:

$$\dot{\rho}_1 = \frac{1-\rho_1^2}{2}[\mu\rho_1 \cos\alpha + p_{\text{switch}}\rho_2 \cos(-\psi - \alpha)] + \xi(t), \tag{8a}$$

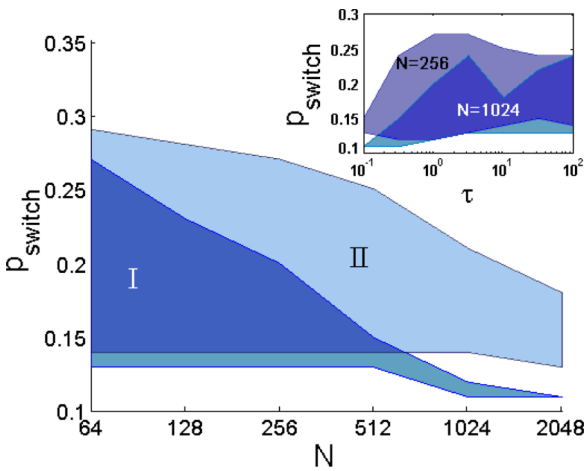

FIG. 7. (Color online) Extent of the region of alternating chimera as a function of the network size for two values of τ. Region I corresponds to $\tau = 0.1$ and region II to $\tau = 10$. Other parameters as in Fig. 1. The inset shows the range of p_{switch} that allows for alternating chimeras as a function of τ for two different values of N ($N = 256$ and $N = 1024$).

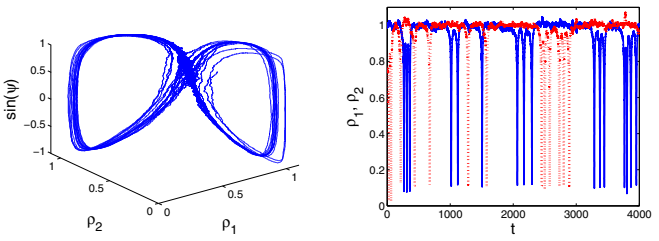

(a) (b)

FIG. 8. (Color online) (a) Phase portrait of Eqs. (8) and (b) time evolution of ρ_1 (blue solid line) and ρ_2 (red dotted line) with $p_{\text{switch}} = 0.25$, $D = 0.004$. Other parameters as in Fig. 1.

$$\dot{\rho}_2 = \frac{1-\rho_2^2}{2}[\mu\rho_2\cos\alpha + p_{\text{switch}}\rho_1\cos(\psi-\alpha)] - \xi(t), \tag{8b}$$

$$\dot{\psi} = -\frac{1+\rho_1^2}{2}\left[\mu\sin\alpha + p_{\text{switch}}\frac{\rho_2}{\rho_1}\sin(\psi+\alpha)\right] + \frac{1+\rho_2^2}{2}\left[\mu\sin\alpha + p_{\text{switch}}\frac{\rho_1}{\rho_2}\sin(-\psi+\alpha)\right], \tag{8c}$$

where $\xi(t)$ is a Gaussian white noise satisfying $\langle\xi(t)\xi(t')\rangle = D\delta(t-t')$ with noise intensity D.

We have numerically verified that a small level of noise in Eqs. (8) leads to alternating chimera states analogous to those observed in the switching system. For instance, the alternating chimera state of Fig. 2(c) is also identified in the averaged reduced model (8) for $p_{\text{switch}} = 0.25$ and $D = 0.004$ (Fig. 8).

To study the dependence of the fluctuations on τ and N, we have performed numerical simulations while monitoring the standard deviation σ_R of the Kuramoto order parameter in Eq. (3) for the desynchronized population of a stable chimera state in dependence on τ at different values of N. The results (not reported) show that fluctuations indeed increase with τ and decrease with N. The consequence is that, increasing τ for large size networks, the range of p_{switch} allowing for alternating chimeras increases, as shown in the inset of Fig. 7.

V. CONCLUSIONS

In this work we have considered a pair of two populations of identical oscillators with time-varying interpopulation links. In the case of fixed connectivity, such a network exhibits stable or breathing chimeras, while alternating chimeras may be observed only if a degree of heterogeneity in the distribution of oscillator intrinsic frequencies is introduced. When the interpopulation links change over time, we have found that the network may support all the three chimera states even in the case of identical oscillators.

The switching between the different network topologies, which result from the stochastic rule used to establish interpopulation links, induces fluctuations in the system. We have found that such fluctuations are averaged out in the thermodynamic limit and under the assumption of small switching intervals. In this case, the dynamics of the system can be qualitatively represented by a low-dimensional averaged system that accurately predicts the stable and breathing chimeras. However, fluctuations are fundamental to explain the onset of alternating chimera states and can be incorporated in the low-dimensional model with the addition of a stochastic term. Since fluctuations increase for decreasing values of N and increasing of τ, alternating chimera states are likely to occur not only in small networks, but also in arbitrary large structures in the presence of large switching time intervals.

Our findings can be generalized for more than two populations coupled in a ring configuration with time-varying interpopulation links. We have evidence that this gives rise to traveling incoherent domains and other spatio-temporal patterns of coherence and incoherence.

Finally, we notice that our results may be related to stochastic resonance or, more in general, to noise-induced phenomena in bistable or excitable systems [40,41]. In our system, the internal noise plays a fundamental role in eliciting the alternating chimera state. We have observed that, depending on the noise level, fluctuations may either regularize the alternating behavior or lead to a very long-tailed distribution of the residence times.

ACKNOWLEDGMENTS

The authors would like to thank Thomas Isele for helpful discussions. P.H. acknowledges support by Deutsche Forschungsgemeinschaft in the framework of SFB 910 and BMBF (Grant No. 01Q1001B) in the framework of BCCN Berlin.

[1] Y. Kuramoto and D. Battogtokh, Nonlinear Phenom. Complex Syst. **5**, 380 (2002).
[2] D. M. Abrams and S. H. Strogatz, Phys. Rev. Lett. **93**, 174102 (2004).
[3] S.-i. Shima and Y. Kuramoto, Phys. Rev. E **69**, 036213 (2004).
[4] D. M. Abrams, R. Mirollo, S. H. Strogatz, and D. A. Wiley, Phys. Rev. Lett. **101**, 084103 (2008).
[5] E. A. Martens, C. R. Laing, and S. H. Strogatz, Phys. Rev. Lett. **104**, 044101 (2010).
[6] A. E. Motter, Nat. Phys. **6**, 164 (2010).
[7] R. Singh and S. Sinha, Phys. Rev. E **87**, 012907 (2013).
[8] L. V. Gambuzza, A. Buscarino, S. Chessari, L. Fortuna, R. Meucci, and M. Frasca, Phys. Rev. E **90**, 032905 (2014).
[9] M. R. Tinsley, S. Nkomo, and K. Showalter, Nat. Phys. **8**, 662 (2012).
[10] I. Omelchenko, Y. Maistrenko, P. Hövel, and E. Schöll, Phys. Rev. Lett. **106**, 234102 (2011).
[11] I. Omelchenko, B. Riemenschneider, P. Hövel, Y. Maistrenko, and E. Schöll, Phys. Rev. E **85**, 026212 (2012).
[12] G. C. Sethia, A. Sen, and G. L. Johnston, Phys. Rev. E **88**, 042917 (2013).
[13] L. Schmidt, K. Schonleber, K. Krischer, and V. Garcia-Morales, Chaos **24**, 013102 (2014).

[14] A. Zakharova, M. Kapeller, and E. Schöll, Phys. Rev. Lett. **112**, 154101 (2014).
[15] G. C. Sethia and A. Sen, Phys. Rev. Lett. **112**, 144101 (2014).
[16] I. Omelchenko, O. E. Omel'chenko, P. Hövel, and E. Schöll, Phys. Rev. Lett. **110**, 224101 (2013).
[17] C. R. Laing, Chaos **22**, 043104 (2012).
[18] N. C. Rattenborg, C. J. Amlaner, and S. L. Lima, Neurosci. Biobehav. Rev. **24**, 817 (2000).
[19] C. G. Mathews, J. A. Lesku, S. L. Lima, and C. J. Amlaner, Ethology **112**, 286 (2006).
[20] O. I. Lyamin, P. R. Manger, S. H. Ridgway, L. M. Mukhametov, and J. M. Siegel, Neurosci. Biobehav. Rev. **32**, 1451 (2008).
[21] R. Ma, J. Wang, and Z. Liu, Europhys. Lett. **91**, 40006 (2010).
[22] J. H. Sheeba, V. K. Chandrasekar, and M. Lakshmanan, Phys. Rev. E **81**, 046203 (2010).
[23] S. W. Haugland, L. Schmidt, and K. Krischer, arXiv:1411.4800
[24] E. A. Martens, Chaos **20**, 043122 (2010).
[25] E. A. Martens, Phys. Rev. E **82**, 016216 (2010).
[26] A. M. Hagerstrom, T. E. Murphy, R. Roy, P. Hövel, I. Omelchenko, and E. Schöll, Nat. Phys. **8**, 658 (2012).
[27] E. A. Martens, S. Thutupalli, A. Fourrire, and O. Hallatschek, Proc. Natl. Acad. Sci. USA **110**, 10563 (2013).
[28] P. Holme and J. Saramki, Phys. Rep. **519**, 97 (2012).
[29] M. Porfiri, D. J. Stilwell, E. M. Bollt, and J. D. Skufca, Physica D: Nonlinear Phenom. **224**, 102 (2006).
[30] I. V. Belykh, V. N. Belykh, and M. Hasler, Physica D: Nonlinear Phenom. **195**, 188 (2004).
[31] M. Porfiri, Phys. Rev. E **85**, 056114 (2012).
[32] E. Montbrió, J. Kurths, and B. Blasius, Phys. Rev. E **70**, 056125 (2004).
[33] E. Barreto, B. Hunt, E. Ott, and P. So, Phys. Rev. E **77**, 036107 (2008).
[34] E. Ott and T. M. Antonsen, Chaos **18**, 037113 (2008).
[35] J. G. Restrepo and E. Ott, Europhys. Lett. **107**, 60006 (2014).
[36] P. So, B. C. Cotton, and E. Barreto, Chaos **18**, 037114 (2008).
[37] A. Pikovsky and M. G. Rosenblum, Phys. Rev. Lett. **101**, 264103 (2008).
[38] P. S. Skardal and J. G. Restrepo, Phys. Rev. E **85**, 016208 (2012).
[39] M. Hasler, V. Belykh, and I. Belykh, SIAM J. Appl. Dyn. Syst. **12**, 1007 (2013).
[40] L. Gammaitoni, P. Hänggi, P. Jung, and F. Marchesoni, Rev. Mod. Phys. **70**, 223 (1998).
[41] C. S. Zhou, J. Kurths, E. Allaria, S. Boccaletti, R. Meucci, and F. T. Arecchi, Phys. Rev. E **67**, 066220 (2003).